# Representing aquifer architecture in macrodispersivity models with an analytical solution of the transition probability matrix

Zhenxue Dai,[1] Andrew Wolfsberg,[1] Zhiming Lu,[1] and Robert Ritzi Jr.[2]

[1] The multi-dimensional transition probability model represents hydrofacies architecture in modeling aquifer heterogeneity. The structure of the aquifer architecture is mathematically characterized by a canonical representation of the transition probability matrix, solved by an eigenvalue decomposition method. Whereas the eigenvalue decomposition has been numerically solved previously, we show here that it can be analytically solved under the assumptions that cross-transition probabilities are dictated by facies proportions and that the juxtapositional tendencies of the facies are symmetric. Although limited by the assumptions, analytical solutions provide more immediate insights about the relationships between transition probability and facies proportion and mean length. The analytical solution is first tested by comparison with the numerical solutions and then used to represent hydrofacies architecture within expressions for the spatial covariance of conductivity and the macrodispersivity. The relationship between the longitudinal macrodispersivity and integral scale, the indicator correlation length, and the facies proportion is represented in an equation for estimating the field-scale dispersivity. An example is used to show how sedimentary structures, conductivity contrasts, and facies mean lengths affect the scales of the macrodispersivity. **Citation:** Dai, Z., A. Wolfsberg, Z. Lu, and R. Ritzi Jr. (2007), Representing aquifer architecture in macrodispersivity models with an analytical solution of the transition probability matrix, *Geophys. Res. Lett.*, *34*, L20406, doi:10.1029/2007GL031608.

## 1. Introduction

[2] Markov chains have been applied in geostatistical models for simulating the spatial distribution of geologic units using categorical indicator variables for a few decades [e.g., *Agterberg*, 1974; *Rolke*, 1991; *Politis*, 1994; *Carle and Fogg*, 1997; *Ritzi et al.*, 2004]. In the Markov chain model, both conceptual facies model and quantitative information (proportions, lengths, juxtapositioning frequency) can be combined to mathematically represent facies architecture [*Ritzi*, 2000; *Zhang*, 2002; *Rubin*, 2003; *Ritzi et al.*, 2004; *Dai et al.*, 2004a, 2005]. The structure of the aquifer architecture is mathematically characterized by a canonical representation of the transition-probability matrix, solved by an eigenvalue decomposition method, which previously has been solved numerically [e.g., *Carle and Fogg*, 1997]. The

analytical decomposition described here allows us to create a mathematical framework in which the Markov chain model representation of geologic architecture is incorporated into the Lagrangian-based, analytical expressions for the macrodispersion of inert solutes. Deriving the macrodispersion equations or upscaling other flow and solute transport parameters in closed form requires exact solutions or analytical functions to express the transition probability model [*Rubin*, 1995; *Ritzi et al.*, 2004]. Although sometimes limited by various assumptions, analytical models generally provide more immediate insights about the relationships between state variables and model parameters. *Lu and Zhang* [2002] derived an analytical solution of transition probability from a Markov chain model for bimodal sediments. For multimodal distributions, *Ritzi and Allen-King* [2007] and *Dai et al.* [2004b, 2007] gave empirical relationships between transition probability functions and the proportions and geometric attributes of facies.

[3] In this article, we first develop an analytical representation for hydrofacies architecture through a solution for the eigenvalue decomposition of the transition rate matrix and the development of the spectral component matrices (using Sylvester's theorem [*Agterberg*, 1974]). To show that the assumptions we are required to make are robust, we compare the analytical solution with both the numerical results and the sample transition probabilities taken from a field case. Second, the Markov chain model is used to represent hydrofacies architecture in a spatial covariance model, which is incorporated into an analytical expression for the pre-asymptotic macrodispersion of inert solutes based on the Lagrangian approach [*Dagan*, 1989; *Gelhar*, 1993]. Through this development, using the analytical formulation, we can directly link the spreading of inert solutes to the Markov chain model and the aquifer architecture. This provides an efficient framework for evaluation how indicator correlation lengths, conductivity integral scales, and facies proportions and mean lengths all contribute to plume spreading.

## 2. Analytical Solution of Facies Transition Probability

### 2.1. Continuous-Lag Multidimensional Markov Chain Model

[4] Consider a domain consisting of N facies in mutually exclusive occurrences. The transition probability $t_{ki}(\boldsymbol{h}_\phi)$, which represents the volumetric proportions, geometry and juxtapositional tendencies of the facies, is given by *Ross* [1988],

$$t_{ki}(\boldsymbol{h}_\phi) = \Pr\{I_k(\boldsymbol{x}') = 1 \text{ and } I_i(\boldsymbol{x}) = 1\}/\Pr\{I_k(\boldsymbol{x}) = 1\},$$

[1]Earth and Environmental Sciences Division, Los Alamos National Laboratory, Los Alamos, New Mexico, USA.
[2]Department of Earth and Environmental Sciences, Wright State University, Dayton, Ohio, USA.

where $\boldsymbol{h}_\phi$ is the lag distance between two points $\boldsymbol{x}$ and $\boldsymbol{x}'$ in direction $\phi$ and $I_k(\mathbf{x})$ is the indicator spatial function for facies $k$. In a three-dimensional transition probability model, the spatial variability of facies distributions in direction $\phi$ can be characterized by a one-dimensional Markov chain model [*Agterberg*, 1974; *Politis*, 1994; *Carle and Fogg*, 1997; *Lu and Zhang*, 2002]. The continuous-lag transition probability matrix $\mathbf{T}$ in direction $\phi$ is written as:

$$\mathbf{T}(\boldsymbol{h}_\phi) = \left(t_{ki}(\boldsymbol{h}_\phi)\right)_{N \times N} = e^{\mathbf{R}\boldsymbol{h}_\phi} \qquad (1)$$

where $\mathbf{R} = (r_{ki})_{N \times N}$ is an $N \times N$ transition rate matrix whose entries $r_{kj}$ denote conditional rates of change per unit length from category $k$ to category $i$ in the direction $\phi$.

[5] If $\mathbf{R}$ is known, the transition probability matrix $\mathbf{T}$ can be evaluated by eigenvalue analyses. Let $\eta_j$, $j = \overline{1, N}$ be distinct eigenvalues of the transition rate matrix $\mathbf{R}$, and $\mathbf{Z}_j$, $j = \overline{1, N}$ be their corresponding spectral component matrices, which are computed by

$$\mathbf{Z}_j = \prod_{m \neq j} (\eta_m \mathbf{I} - \mathbf{R}) \bigg/ \prod_{m \neq j} \left(\eta_m - \eta_j\right), \qquad (2)$$

where $\mathbf{I}$ is the $N \times N$ identity matrix. Note that if $\eta_m \approx \eta_j$, equation (2) would have numerical problems because the denominator is close to zero. The transition probability matrix can be expressed as [*Agterberg*, 1974]

$$\mathbf{T}(\boldsymbol{h}_\phi) = \sum_{j=1}^{N} e^{\eta_j \boldsymbol{h}_\phi} \mathbf{Z}_j. \qquad (3)$$

[6] Whereas the eigenvalues and spectral component matrices in equation (2) were solved numerically by *Carle and Fogg* [1997], we develop here a closed-form analytical solution to the eigenvalues and spectral component matrices for expressing the relationship between the Markov chain model and plume spreading. Furthermore, we have found that in some cases an analytical solution will be helpful to avoid the numerical difficulties that can occur when eigenvalues in equation (2) are similar.

## 2.2. Analytical Solution of Facies Transition Probability

[7] In order to obtain an analytical formulation of the transition probability, we first assume that cross-transition (across facies) probabilities depend on facies volumetric proportions ($p_k$, $k = \overline{1, N}$) only, in which case the off-diagonal transition probabilities $t_{ki}(\boldsymbol{h}_\phi)$ are [*Carle and Fogg*, 1997]:

$$t_{ki}(\boldsymbol{h}_\phi) = \left[1 - t_{kk}(\boldsymbol{h}_\phi)\right] \frac{p_i}{1 - p_k} \quad \text{for} \quad i \neq k. \qquad (4)$$

In making this assumption, we cannot strictly represent some geologic scenarios, like fining upwards sequences. Differentiating equation (4) with respect to $\boldsymbol{h}_\phi$ at $\boldsymbol{h}_\phi = 0$, the off-diagonal transition rates can be computed from diagonal transition rates as

$$r_{ki} = \frac{-r_{kk} p_i}{(1 - p_k)}, \quad i \neq k, \qquad (5)$$

and the rate matrix $\mathbf{R}$ becomes,

$$\mathbf{R} = \begin{bmatrix} r_{11} & \dfrac{-r_{11} p_2}{(1 - p_1)} & \cdots & \dfrac{-r_{11} p_N}{(1 - p_1)} \\ \dfrac{-r_{22} p_1}{(1 - p_2)} & r_{22} & \cdots & \dfrac{-r_{22} p_N}{(1 - p_2)} \\ \vdots & \vdots & \ddots & \vdots \\ \dfrac{-r_{NN} p_1}{(1 - p_N)} & \dfrac{-r_{NN} p_2}{(1 - p_N)} & \cdots & r_{NN} \end{bmatrix}. \qquad (6)$$

Secondly, we assume that the juxtapositional tendencies between categories $k$ and $i$ are symmetric in the direction $\phi$. The assumption of symmetry does not necessarily require that the geometric distribution of categories $k$ and $i$ are symmetric, but only requires that $t_{ki}(\boldsymbol{h}_{+\phi}) = t_{ki}(\boldsymbol{h}_{-\phi})$ [*Carle and Fogg*, 1997], so that the cross-transition probabilities at the symmetric positions, such as $t_{ik}$ and $t_{ki}$, satisfy

$$p_k t_{ki}(\boldsymbol{h}_\phi) = p_i t_{ik}(\boldsymbol{h}_\phi), \quad \text{and} \quad r_{ki} = r_{ik} \, p_i / p_k, \quad \text{for} \quad i \neq k. \qquad (7)$$

Substituting $r_{ki}$ in equation (7) into equation (5), we have

$$r_{ki} = \frac{-r_{kk} p_i}{(1 - p_k)} = \frac{p_i}{p_k} \frac{-r_{ii} p_k}{(1 - p_i)}, \quad \text{or} \quad \frac{r_{kk}}{(1 - p_k)} = \frac{r_{ii}}{(1 - p_i)}, \quad i \neq k. \qquad (8)$$

By using equation (8), we can rewrite the transition rate matrix as

$$\mathbf{R} = \frac{-r_{11}}{(1 - p_1)} \begin{bmatrix} p_1 - 1 & p_2 & \cdots & p_N \\ p_1 & p_2 - 1 & \cdots & p_N \\ \vdots & \vdots & \ddots & \vdots \\ p_1 & p_2 & \cdots & p_N - 1 \end{bmatrix}. \qquad (9)$$

Letting $\dfrac{-r_{11}}{(1 - p_1)} = \dfrac{1}{\lambda_I}$, we compute the eigenvalues of $\mathbf{R}$ by using $\det|\mathbf{R} - \eta \mathbf{I}| = 0$ or

$$\begin{vmatrix} p_1 - 1 - \lambda_I \eta & p_2 & \cdots & p_N \\ p_1 & p_2 - 1 - \lambda_I \eta & \cdots & p_N \\ \vdots & \vdots & \ddots & \vdots \\ p_1 & p_2 & \cdots & p_N - 1 - \lambda_I \eta \end{vmatrix} = 0. \qquad (10)$$

By applying properties of determinants for row and column operations and $\sum_{i=1}^{N} p_i = 1$, equation (10) simplifies to

$$\begin{vmatrix} -1 - \lambda_I \eta & 0 & \cdots & 0 \\ 0 & -1 - \lambda_I \eta & \cdots & 0 \\ \vdots & \vdots & \ddots & \vdots \\ p_1 & p_2 & \cdots & -\lambda_I \eta \end{vmatrix} = 0. \qquad (11)$$

From equation (11) we have the final equation, $\eta(1 + \lambda_I \eta)^{N-1} = 0$, and the matrix $\mathbf{R}$ has eigenvalues $\eta_1 = 0$, and $(N - 1)$ repeated eigenvalues $\eta_2 = -1/\lambda_I$. Then, we compute spectral component matrices with equation (2) as $\mathbf{Z}_1 = (p_1, p_2, \ldots, p_N)_{1 \times N}$, $\mathbf{Z}_2 = (\delta_{ki} - p_i)_{N \times N}$, where $\delta_{ki}$ is the Kronecker delta. Substituting into (3) with the computed

**Table 1.** Sediment Lithofacies and Their Statistics in the Vertical Direction

| Lithofacies | $k$ | Proportion | Mean Thickness, m | $\lambda_{I\,k,\phi} = \overline{L}_{k,\phi}(1 - p_k)$, m |
|---|---|---|---|---|
| Debris flow | 1 | 0.07 | 1.32 | 1.23 |
| Floodplain | 2 | 0.56 | 2.52 | 1.11 |
| Levee | 3 | 0.19 | 1.53 | 1.24 |
| Channel | 4 | 0.18 | 1.52 | 1.25 |

eigenvalues and spectral component matrices, we obtain the analytical solution of the transition probability as

$$t_{ki}(\boldsymbol{h}_\phi) = p_i + (\delta_{ki} - p_i)e^{-\frac{h_\phi}{\lambda_I}} \qquad (k,\, i = \overline{1, N}), \qquad (12)$$

where $\lambda_I$ is the indicator correlation length. For $k = i$, the auto-transition probability is

$$t_{kk}(\boldsymbol{h}_\phi) = p_k + (1 - p_k)e^{-\frac{h_\phi}{\lambda_I}}. \qquad (13)$$

The mean length $\overline{L}_{k,\phi}$ of a facies $k$ along lines in the direction $\phi$ can be computed as [*Carle and Fogg*, 1997]

$$\left. \frac{\partial t_{kk}(\boldsymbol{h}_\phi)}{\partial \boldsymbol{h}_\phi} \right|_{\boldsymbol{h}_\phi \to 0+} = -\frac{1}{\lambda_I}(1 - p_k) = -\frac{1}{\overline{L}_{k,\phi}} \qquad (14)$$

Therefore, $\lambda_I = \overline{L}_{k,\phi}(1 - p_k)$. This result indicates that a uniform indicator correlation length exists when the sedimentary facies distributions satisfy the above two assumptions.

### 2.3. An Application to a Field Example

[8] Here the analytical solution is tested with a field example for which a numerically-developed Markov chain model has been published [*Carle and Fogg*, 1997]. The purpose of comparing the analytical solution to the numerical solution is to illustrate differences in the Markov chain model that may result from our assumptions. The field site is located at Lawrence Livermore National Laboratory (LLNL) near the Southeast end of the Livermore Valley. The Livermore Valley is relatively flat, underlain by a complex alluvial sedimentary basin drained by two intermittent streams. LLNL drilled over 350 boreholes for characterizing the subsurface sedimentary structures. The subsurface unconsolidated alluvial sediments were categorized with the data interpreted from cores, textural descriptions, and geophysical logs. Table 1 lists the proportions and thicknesses for each of the four hydrofacies.

[9] Using equation (14), we compute the indicator correlation lengths for each facies and also list them in Table 1. Note that the mean lengths of the facies are measured vertically down boreholes and are slightly larger than those measured perpendicularly to the dips of the facies. The correlation lengths computed for each facies are not exactly the same because the assumption of symmetry is not strictly met by the data analysis. Yet, they are similar and to develop the Markov chain model, we take the volume average:

$$\lambda_I = \sum_{k=1}^{N} p_k \lambda_{I\,k,\phi} = \sum_{k=1}^{N} p_k \overline{L}_{k,\phi}(1 - p_k), \qquad (15)$$

which gives $\lambda_I = 1.2$ m. With this indicator correlation length and the volumetric proportion data, we compute analytically the Markov chain model in the vertical direction using equation (12) and for the purpose of comparison, we plot it together with the sample transition probability and the numerical results of *Carle and Fogg* [1997] in Figure 1. In most cases, the asymptotic exponential function of the analytical transition probability model is a good representation of the auto- and cross-transition probabilities. The biggest difference is in the case of transition from channel facies to levee facies. The shape of the sample transition probability from channel to levee is not simply exponential as in random associations. Furthermore, the transition probability for levee to channel is not symmetric. Levee facies usually occur adjacent to and above channel facies, rather than in random association with the facies. The analytical solution cannot represent this association for these two facies. The generally favorable comparison builds confidence that the analytical solution for the transition probability model has significant applicability, despite the underlying assumptions. Given the well-defined closed-formed expression of equation (12), we can use it to evaluate models of conductivity covariance, and macrodispersion.

## 3. Conductivity Covariance Function Incorporating the Markov Chain Model

[10] Let $Y(\boldsymbol{x})$ be the spatial random function of log-conductivity, which can be divided into subpopulations according to facies as per *Rubin* [1995],

$$Y(\boldsymbol{x}) = \sum_{k=1}^{N} I_k(\boldsymbol{x}) Y_k(\boldsymbol{x}), \qquad (16)$$

where $Y_k(\boldsymbol{x})$ represents log-conductivity within facies $k$. According to *Ritzi et al.* [2004], the composite covariance $C_Y(\boldsymbol{h}_\phi)$ of $Y(\boldsymbol{x})$ can be represented in terms of proportion, transition probability, and the in-unit or cross-unit covariance of $Y_k(\boldsymbol{x})$ as

$$C_Y(\boldsymbol{h}_\phi) = \sum_{k=1}^{N} \sum_{i=1}^{N} \left\{ C_{ki}(\boldsymbol{h}_\phi) + m_k m_i \right\} p_k t_{ki}(\boldsymbol{h}_\phi) - M_y^2, \qquad (17)$$

where $m_k$ and $\sigma_k^2$ denote the mean and variance of $Y_k(\boldsymbol{x})$; $M_Y$ is the composite mean of $Y(\boldsymbol{x})$.

[11] By assuming that the cross-covariances are negligible, i.e., $C_{ki}(\boldsymbol{h}_\phi) = 0$ for $k \neq i$, and applying the analytical solution in equation (12) for transition probability and exponential functions for auto-covariance $C_{kk}(\boldsymbol{h}_\phi)$ [see *Rubin*, 1995; *Dai et al.*, 2004a], we obtain the composite covariance function as

$$C_Y(\boldsymbol{h}_\phi) = \sum_{k=1}^{N} p_k^2 \sigma_k^2 e^{-\frac{h_\phi}{\lambda_k}} + \sum_{k=1}^{N} p_k(1 - p_k)\sigma_k^2 e^{-\frac{h_\phi}{\lambda_\psi}}$$

$$+ \frac{1}{2} \sum_{k=1}^{N} \sum_{i=1}^{N} (m_k - m_i)^2 p_k p_i e^{-\frac{h_\phi}{\lambda_I}}, \qquad (18)$$
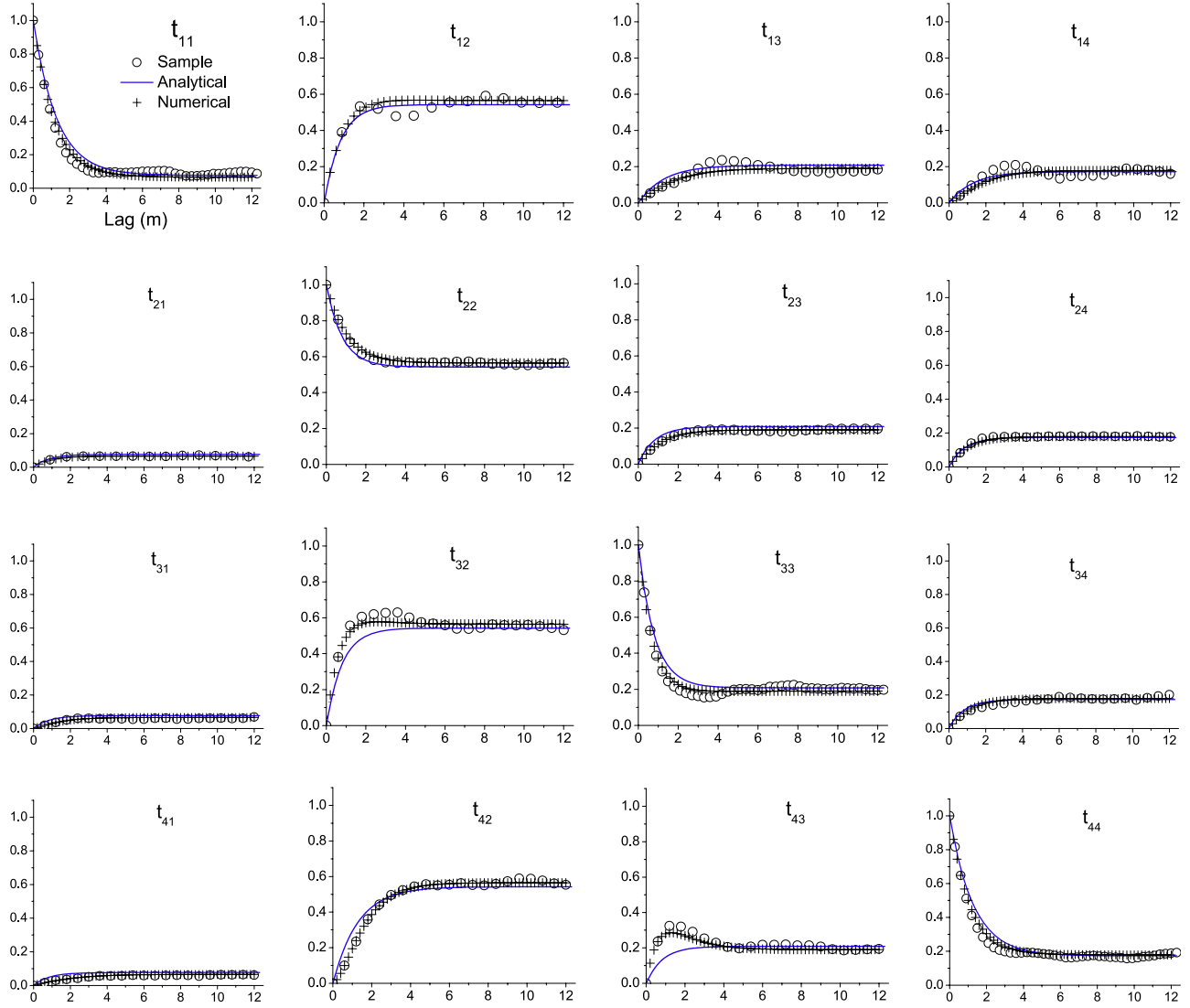
**Figure 1.** Comparison of sample transition probability with analytical and numerical solutions.

where $\lambda_\psi = \lambda_k \lambda_I / (\lambda_k + \lambda_I)$ and $\lambda_k$ is the integral scale of log conductivity in facies $k$.

## 4. Macrodispersivity Model

[12] To derive the macrodispersivity equations, we use the same assumptions as *Rubin* [1995]: (1) the flow field is at steady state, (2) the conductivity field is weakly stationary, (3) the velocity field is uniform in the mean, (4) the flow domain is unbounded, and (5) the variance of the log conductivity is smaller than unity. Furthermore, assuming that the mean displacement velocity of a solute particle is approximated at the first order by the average fluid velocity, the macrodispersion coefficients are computed by:

$$D_{jl}(t) = \int_0^t u_{jl}(U_1 t') dt' \tag{19}$$

where $D_{jl}(t)$ is the macroscopic dispersivity tensor, $u_{jl}$ is the velocity covariance, and $U_1$ is the mean velocity. Following *Rubin* [1995] and replacing the bimodal covariance function with the multimodal covariance of equation (18), we derived the longitudinal and transverse macrodispersion coefficients in the three-dimensional domain as

$$\frac{D_{11}(t)}{U_1} = \sum_{k=1}^N \sigma_k^2 p_k \left( p_k \lambda_k A(\tau_1) + \left(1 - p_k\right) \lambda_\psi A(\tau_2) \right. $$
$$\left. + \frac{\lambda_I}{2\sigma_k^2} A(\tau_3) \sum_{i=1}^N p_i (m_k - m_i)^2 \right), \tag{20}$$

$$\frac{D_{22}(t)}{U_1} = \sum_{k=1}^N \sigma_k^2 p_k \left( p_k \lambda_k B(\tau_1) + (1 - p_k) \lambda_\psi B(\tau_2) \right. $$
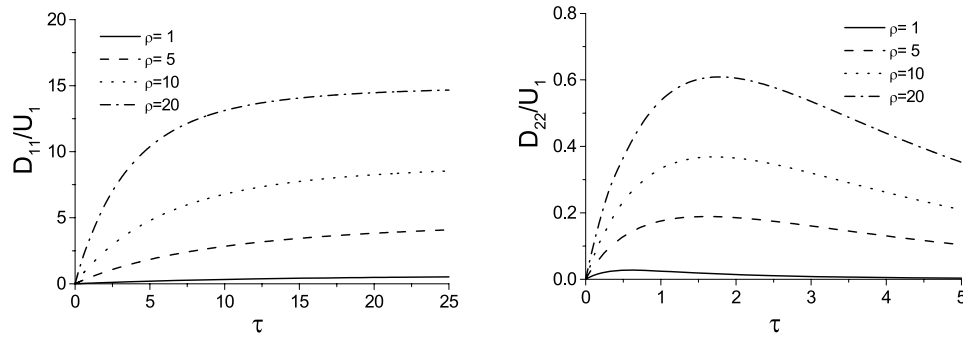$$\left. + \frac{\lambda_I}{2\sigma_k^2} B(\tau_3) \sum_{i=1}^N p_i (m_k - m_i)^2 \right), \tag{21}$$

**Figure 2.** Sensitivity of the longitudinal and transverse macrodispersion coefficients to conductivity contrast ($\rho = \overline{K}_{max}/\overline{K}_{min}$) in the three-dimensional domain ($\tau = U_1 t/\lambda_I$).

where, $A(\tau_i) = 1 + \dfrac{4}{e^{\tau}\tau_i^4}\left[6(e^{\tau_i} - \tau_i - 1) - \tau_i^2(e^{\tau_i} + 2)\right]$, $\tau_i$ is the dimensionless time expressed as $\tau_1 = tU_1/\lambda_k$, $\tau_2 = tU_1/\lambda_\psi$, $\tau_3 = tU_1/\lambda_I$, and $B(\tau_i) = \dfrac{1}{e^{\tau}\tau_i^4}\left[12(1 + \tau_i - e^{\tau_i}) + \tau_i^2(5 + e^{\tau_i} + \tau_i)\right]$.

[13] Equations (20) and (21) relate the macrodispersion coefficients to the facies statistical parameters such as the facies proportion and correlation length, and the variance and mean of log conductivity. The macrodispersion coefficients are positively correlated with the mean difference (or the contrast) of log conductivity. Figure 2 shows the macrodispersion coefficients increase with the increasing conductivity contrast, which is defined as $\rho = \overline{K}_{max}/\overline{K}_{min}$, where $\overline{K}_{max}$ and $\overline{K}_{min}$ are the maximum and minimum geometric means of conductivity within the $N$ facies ($\overline{K}_i = e^{m_i}, i = \overline{1, N}$). When $\rho = 1$, the third term (also called the cross-facies-transition term) in (20) and (21) is zero and the macrodispersion coefficients only consist of the first two terms (also called the auto-transition terms or within-facies-transition). When $\rho$ increases, the contribution of the cross-transition term to the macrodispersion increases. When $\rho \geq 10$, the cross-transition term dominates over the auto-transition terms. The results in Figure 2 indicate that the variation of conductivity within and across facies is the source of the macrodispersion and in a homogeneous aquifer system the macrodispersion coefficients are zero.

[14] When time is sufficiently large, the transverse macrodispersivity approaches zero, while the longitudinal macrodispersivity has the following simplified expression,

$$\frac{D_{11}}{U_1} = \sum_{k=1}^{N} \sigma_k^2 p_k \left(p_k\lambda_k + (1 - p_k)\lambda_\psi + \frac{\lambda_I}{2\sigma_k^2}\sum_{i=1}^{N} p_i(m_k - m_i)^2\right). \tag{22}$$

Equation (22) shows how different modes of variability in log conductivity contribute to the macrodispersion at the later time. For a unimodal distribution of facies, $N = 1$, equation (22) becomes $D_{11}/U_1 = \sigma^2\lambda$, which is the same as the unimodal macrodispersivity derived by *Dagan* [1989] and *Gelhar* [1993]. Equation (22) provides a way to estimate the longitudinal macrodispersivity of a multimodal conductivity field from the facies proportions, mean and variance of log conductivity in each facies, and the indicator correlation length.

[15] In order to analyze the impact of facies mean lengths on macrodispersion with equation (22), we create a set of synthetic data of log conductivity (Table 2), and use them to estimate the longitudinal macrodispersion coefficients with variable mean length of the floodplain. When we vary the mean length of floodplain from 1 to 30 m and fix other parameters, we find a linear relationship among the mean length of the floodplain, the indicator correlation length, and the macrodispersivity (see Figure 3), which means the macrodispersivity increases with the increasing mean lengths of the facies.

## 5. Conclusions

[16] The analytical eigenvalue decomposition in formulating a Markov chain model for aquifer architecture allows us to derive the associated macrodispersion coefficients for solute transport in a three-dimensional domain. This, in turn, facilitates analyzing the link between aquifer architecture and plume spreading. We can easily and independently
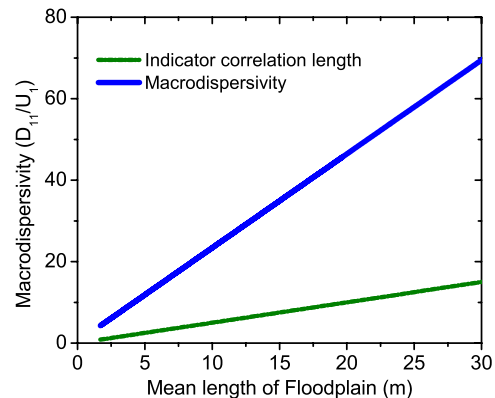
**Table 2.** Mean, Variance, and Correlation Length of Synthetic Data of Log-Conductivity for the Lithofacies[a]

| Lithofacies | $k$ | $m_k$ | $\sigma_k^2$ | $\lambda_k$ |
|---|---|---|---|---|
| Debris flow | 1 | −0.84 | 0.2 | 0.9 |
| Floodplain | 2 | −3.14 | 0.5 | 1.0 |
| Levee | 3 | −1.76 | 0.3 | 1.2 |
| Channel | 4 | 1.46 | 0.55 | 1.1 |

[a]Log-Conductivity, m/d.



**Figure 3.** Facies mean length vs. indicator correlation length and macrodispersivity.

analyze the relative contributions of facies proportions, mean lengths, in-facies variance and per-facies covariance in log-conductivity, and the difference in mean log-conductivity across facies. At late time, the longitudinal dispersivity coefficient clearly shows a linear dependence on the variance of log conductivity, the mean length of facies and the indicator correlation length.

## References

Agterberg, F. P. (1974), *Geomathematics*, 596 pp., Elsevier Sci., New York.

Carle, S. F., and G. E. Fogg (1997), Modeling spatial variability with one- and multi-dimensional continuous Markov chains, *Math. Geol.*, *29*(7), 891–918.

Dagan, G. (1989), *Flow and Transport in Porous Formations*, 465 pp., Springer, New York.

Dai, Z., R. W. Ritzi, C. Huang, D. F. Dominic, and Y. N. Rubin (2004a), Transport in heterogeneous sediments with multimodal conductivity and hierarchical organization across scales, *J. Hydrol.*, *294*, 68–86.

Dai, Z., R. W. Ritzi, and D. F. Dominic (2004b), Estimating parameters for hierarchical permeability correlation models, in *Aquifer Characterization*, edited by J. Bridge and D. Hyndman, *Spec. Publ. SEPM Soc. Sediment. Geol.*, *80*, 41–54.

Dai, Z., R. W. Ritzi Jr., and D. F. Dominic (2005), Improving permeability semivariograms with transition probability models of hierarchical sedimentary architecture derived from outcrop analog studies, *Water Resour. Res.*, *41*, W07032, doi:10.1029/2004WR003515.

Dai, Z., A. Wolfsberg, Z. Lu, and P. Reimus (2007), Upscaling matrix diffusion coefficients for heterogeneous fractured rocks, *Geophys. Res. Lett.*, *34*, L07408, doi:10.1029/2007GL029332.

Gelhar, L. W. (1993), *Stochastic Subsurface Hydrology*, Prentice-Hall, Englewood Cliffs, N. J.

Lu, Z., and D. Zhang (2002), On stochastic modeling of flow in multimodal heterogeneous formations, *Water Resour. Res.*, *38*(10), 1190, doi:10.1029/2001WR001026.

Politis, D. N. (1994), Markov chains in many dimensions, *Adv. Appl. Probab.*, *26*(3), 756–774.

Ritzi, R. W. (2000), Behavior of indicator semivariograms and transition probabilities in relation to the variance in lengths of hydrofacies, *Water Resour. Res.*, *36*(11), 3375–3381.

Ritzi, R. W., Jr., and R. M. Allen-King (2007), Why did *Sudicky* [1986] find an exponential-like spatial correlation structure for hydraulic conductivity at the Borden research site?, *Water Resour. Res.*, *43*, W01406, doi:10.1029/2006WR004935.

Ritzi, R. W., Z. Dai, D. F. Dominic, and Y. N. Rubin (2004), Spatial correlation of permeability in cross-stratified sediment with hierarchical architecture, *Water Resour. Res.*, *40*, W03513, doi:10.1029/2003WR002420.

Rolke, W. A. (1991), Continuous-time Markov processes as a stochastic model for sedimentation, *Math. Geol.*, *23*(3), 297–304.

Ross, S. (1988), *A First Course in Probability*, 420 pp., Macmillan, New York.

Rubin, Y. (1995), Flow and transport in bimodal heterogeneous formations, *Water Resour. Res.*, *31*(10), 1468–2461.

Rubin, Y. (2003), *Applied Stochastic Hydrogeology*, Oxford Univ. Press, New York.

Zhang, D. (2002), *Stochastic Methods for Flow in Porous Media: Coping With Uncertainties*, 350 pp., Academic, San Diego, Calif.

―――――――――――

Z. Dai, Z. Lu, and A. Wolfsberg, Earth and Environmental Sciences Division, Los Alamos National Laboratory, EES-6, T003, Los Alamos, NM 87545, USA. (daiz@lanl.gov)

R. Ritzi Jr., Department of Earth and Environmental Sciences, Wright State University, Dayton, OH 45435, USA.